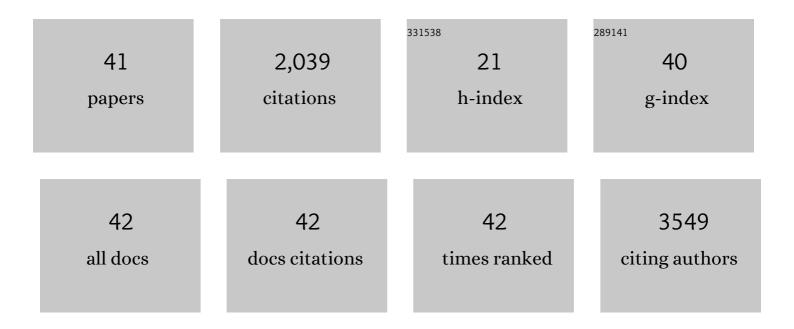
Yun-Ru Chen

List of Publications by Year in descending order

Source: https://exaly.com/author-pdf/5552475/publications.pdf Version: 2024-02-01



YUN-RU CHEN

#	Article	IF	CITATIONS
1	Negatively Charged Gold Nanoparticles Inhibit Alzheimer's Amyloidâ€Î² Fibrillization, Induce Fibril Dissociation, and Mitigate Neurotoxicity. Small, 2012, 8, 3631-3639.	5.2	281
2	Distinct Early Folding and Aggregation Properties of Alzheimer Amyloid-β Peptides Aβ40 and Aβ42. Journal of Biological Chemistry, 2006, 281, 24414-24422.	1.6	188
3	Distinct Effects of Zn2+, Cu2+, Fe3+, and Al3+ on Amyloid-β Stability, Oligomerization, and Aggregation. Journal of Biological Chemistry, 2011, 286, 9646-9656.	1.6	176
4	Full-length TDP-43 forms toxic amyloid oligomers that are present in frontotemporal lobar dementia-TDP patients. Nature Communications, 2014, 5, 4824.	5.8	153
5	In vitro prion-like behaviour of TDP-43 in ALS. Neurobiology of Disease, 2016, 96, 236-247.	2.1	118
6	Zinc ion rapidly induces toxic, off-pathway amyloid-β oligomers distinct from amyloid-β derived diffusible ligands in Alzheimer's disease. Scientific Reports, 2018, 8, 4772.	1.6	104
7	Amyloid-Beta (Aî²) D7H Mutation Increases Oligomeric Aî²42 and Alters Properties of Aî²-Zinc/Copper Assemblies. PLoS ONE, 2012, 7, e35807.	1.1	94
8	The Truncated C-terminal RNA Recognition Motif of TDP-43 Protein Plays a Key Role in Forming Proteinaceous Aggregates. Journal of Biological Chemistry, 2013, 288, 9049-9057.	1.6	84
9	The Glycine-Alanine Dipeptide Repeat from C9orf72 Hexanucleotide Expansions Forms Toxic Amyloids Possessing Cell-to-Cell Transmission Properties. Journal of Biological Chemistry, 2016, 291, 4903-4911.	1.6	73
10	Removal of the Pro-Domain Does Not Affect the Conformation of the Procaspase-3 Dimer. Biochemistry, 2001, 40, 14224-14235.	1.2	72
11	Distinct responses of neurons and astrocytes to TDP-43 proteinopathy in amyotrophic lateral sclerosis. Brain, 2020, 143, 430-440.	3.7	68
12	Amyloid Oligomer Conformation in a Group of Natively Folded Proteins. PLoS ONE, 2008, 3, e3235.	1.1	63
13	Neuroprotective Effect of the Marine-Derived Compound 11-Dehydrosinulariolide through DJ-1-Related Pathway in In Vitro and In Vivo Models of Parkinson's Disease. Marine Drugs, 2016, 14, 187.	2.2	55
14	TDP-43 interacts with amyloid-β, inhibits fibrillization, and worsens pathology in a model of Alzheimer's disease. Nature Communications, 2020, 11, 5950.	5.8	45
15	The coexistence of an equal amount of Alzheimer's amyloidâ€Î² 40 and 42 forms structurally stable and toxic oligomers through a distinct pathway. FEBS Journal, 2014, 281, 2674-2687.	2.2	43
16	A robust TDP-43 knock-in mouse model of ALS. Acta Neuropathologica Communications, 2020, 8, 3.	2.4	43
17	Folding stability of amyloidâ€Î² 40 monomer is an important determinant of the nucleation kinetics in fibrillization. FASEB Journal, 2011, 25, 1390-1401.	0.2	41
18	Discovery of Dihydrochalcone as Potential Lead for Alzheimer's Disease: In Silico and In Vitro Study. PLoS ONE, 2013, 8, e79151.	1.1	33

Yun-Ru Chen

#	Article	IF	CITATIONS
19	Temperature-Dependent Structural Changes of Parkinson's Alpha-Synuclein Reveal the Role of Pre-Existing Oligomers in Alpha-Synuclein Fibrillization. PLoS ONE, 2013, 8, e53487.	1.1	30
20	Alzheimer's Amyloid-β Oligomers Rescue Cellular Prion Protein Induced Tau Reduction via the Fyn Pathway. ACS Chemical Neuroscience, 2013, 4, 1287-1296.	1.7	26
21	Detection of TDPâ€43 oligomers in frontotemporal lobar degeneration–TDP. Annals of Neurology, 2015, 78, 211-221.	2.8	24
22	Alzheimer's amyloid-β A2T variant and its N-terminal peptides inhibit amyloid-β fibrillization and rescue the induced cytotoxicity. PLoS ONE, 2017, 12, e0174561.	1.1	24
23	Membrane roughness as a sensitive parameter reflecting the status of neuronal cells in response to chemical and nanoparticle treatments. Journal of Nanobiotechnology, 2016, 14, 9.	4.2	21
24	Lipid-Modified Graphene-Transistor Biosensor for Monitoring Amyloid-Î ² Aggregation. ACS Applied Materials & Interfaces, 2018, 10, 12311-12316.	4.0	21
25	Molecular Structure of Amyloid Fibrils Formed by Residues 127 to 147 of the Human Prion Protein. Chemistry - A European Journal, 2010, 16, 5492-5499.	1.7	20
26	Kinetic traps in the folding/unfolding of procaspase-1 CARD domain. Protein Science, 2004, 13, 2196-2206.	3.1	19
27	Alzheimer's Amyloid-β Sequesters Caspase-3 in Vitro via Its C-Terminal Tail. ACS Chemical Neuroscience, 2016, 7, 1097-1106.	1.7	17
28	Equilibrium and Kinetic Folding of a α-Helical Greek Key Protein Domain: Caspase Recruitment Domain (CARD) of RICK. Biochemistry, 2003, 42, 6310-6320.	1.2	16
29	A novel method for expression and purification of authentic amyloid-Î ² with and without 15N labels. Protein Expression and Purification, 2015, 113, 63-71.	0.6	11
30	Discovery of DNA dyes Hoechst 34580 and 33342 as good candidates for inhibiting amyloid beta formation: in silico and in vitro study. Journal of Computer-Aided Molecular Design, 2016, 30, 639-650.	1.3	11
31	Rationally designed divalent caffeic amides inhibit amyloid-β fibrillization, induce fibril dissociation, and ameliorate cytotoxicity. European Journal of Medicinal Chemistry, 2018, 158, 393-404.	2.6	11
32	TAR DNAâ€binding protein 43 oligomers in physiology and pathology. IUBMB Life, 2022, 74, 794-811.	1.5	10
33	Substitutions of prolines examine their role in kinetic trap formation of the caspase recruitment domain (CARD) of RICK. Protein Science, 2006, 15, 395-409.	3.1	9
34	Using optical profilometry to characterize cell membrane roughness influenced by amyloid-beta 42 aggregates and electric fields. Journal of Biomedical Optics, 2013, 19, 011009.	1.4	8
35	Functional Assessment of Residues in the Amino- and Carboxyl-Termini of Crustacean Hyperglycemic Hormone (CHH) in the Mud Crab Scylla olivacea Using Point-Mutated Peptides. PLoS ONE, 2015, 10, e0134983.	1.1	8
36	Acute-phase serum amyloid A for early detection of hepatocellular carcinoma in cirrhotic patients with low AFP level. Scientific Reports, 2022, 12, 5799.	1.6	6

Yun-Ru Chen

#	Article	IF	CITATIONS
37	Time-Evolved SERS Signatures of DEP-Trapped Aβ and Zn ²⁺ Aβ Peptides Revealed by a Sub-10 nm Electrode Nanogap. Analytical Chemistry, 2021, 93, 16320-16329.	3.2	5
38	1H, 15N and 13C resonance assignments of light organ-associated fatty acid-binding protein of Taiwanese fireflies. Biomolecular NMR Assignments, 2016, 10, 71-74.	0.4	3
39	Structure-Based Functional Analysis of a Hormone Belonging to an Ecdysozoan Peptide Superfamily: Revelation of a Common Molecular Architecture and Residues Possibly for Receptor Interaction. International Journal of Molecular Sciences, 2021, 22, 11142.	1.8	1
40	Amyloidâ€Î²40 <scp>E22K</scp> fibril in familial Alzheimer's disease is more thermostable and susceptible to seeding. IUBMB Life, 2022, 74, 739-747.	1.5	1
41	Effects of Dissolved Gases on the Amyloid Fibril Morphology. Langmuir, 2021, 37, 516-523.	1.6	1